An In Situ SAXS/WAXS/Raman Spectroscopy Study on the Phase Behavior of Syndiotactic Polystyrene (sPS)/Solvent Systems: Compound Formation and Solvent (Dis)ordering

S. Rastogi,* J. G. P. Goossens, and P. J. Lemstra

Eindhoven Polymer Laboratories/The Dutch Polymer Institute (DPI), Eindhoven University of Technology, P.O. Box 513, 5600 MB Eindhoven, The Netherlands

Received August 26, 1997

ABSTRACT: In situ small- and wide-angle X-ray scattering (SAXS and WAXS) experiments combined with Raman spectroscopy and thermal analysis have been performed to study the phase behavior of syndiotactic polystyrene (sPS) solutions. Three different solvents were used, respectively, decalin, benzyl methacrylate, and cyclohexyl methacrylate. When sPS solutions are quenched, gel formation occurs. In these gels sPS adopts a helical conformation that is stabilized by the solvent molecules; in fact, compound formation occurs. From the combined experimental data it was concluded that two different structural modifications exist within the solvent-included helical δ-phase, respectively the δ'-phase, in which the solvent molecules are intercalated and ordered between the phenyl rings of sPS, and a δ''-phase, where the solvent ordering is lost. The so-called γ-phase, the solvent-free helical phase, was not observed in our studies. The transformation from the helical (δ'') phase to the planar zigzag (β) phase occurs via melting and recrystallization. Under specific conditions, the β-phase is metastable, even in its thermodynamically stable region.

I. Introduction

Syndiotactic polystyrene (sPS) is, compared with its isomeric counterpart isotactic polystyrene (iPS), a fast crystallizing polymer possessing a high melting temperature of 275 °C. Only recently[1] has it been possible to obtain a high tacticity during the synthesis of sPS in contrast with iPS, a slow crystallizing polymer, which was in fact the first synthetic stereoregular polymer, prepared by Natta et al. in 1955.[2] Some properties that stimulated the commercial interest in sPS are a high heat resistance, a low water absorption, a good chemical resistance, excellent electrical properties, a low density, and a high dielectric strength. However, the high melting temperature could pose problems with respect to processing. A further drawback to overcome is the low ductility due to the high glass transition temperature, approximately 100 °C, similar to standard atactic polystyrene.

A possible solution to overcome some of these problems could be the use of reactive solvents during processing. In our laboratory, this processing technique was applied for both intractable and tractable polymers.[3−5] The polymer to be processed is dissolved in a reactive solvent at elevated temperatures, and the homogeneous solution is transferred into a mold. Upon polymerization of the reactive solvent in the mold, *phase separation* and *phase inversion* occur and the dissolved polymer becomes the continuous matrix and the "polymerized" solvent is dispersed as a particulate phase. In the case of sPS it has been stated that solvents may intercalate with this polymer, resulting in compound formation.[10−15] If reactive solvents are employed, polymerization of these reactive solvents (monomers) in the sPS/solvent compounds could lead to unique polymer systems. In this paper we present the results concerning the interaction between sPS and various selected reactive solvents (monomers). In a subsequent paper the polymerization will be discussed.

Table 1. Modifications for Syndiotactic Polystyrene (sPS)

phase	conformation	phase	conformation
α	planar zigzag	γ^a	helical
β	planar zigzag	δ^b	helical

[a] Solvent-free. [b] Solvent-included.

Various studies have been dealt with crystallization of stereoregular polystyrene, both from the melt and from solutions. Stereoregular polystyrenes can crystallize into various crystal structures possessing different conformations. For example, iPS crystallizes usually in a (3/1) helical conformation consisting of a regular repetition of trans (T) and gauche (G) conformations of the skeletal C−C bonds,[6] like isotactic polypropylene (iPP), but a (12/1) helix has been reported in the case of iPS gels obtained by cooling iPS/decalin solutions at large supercoolings. This occurrence of a (12/1) helix in the case of iPS, however, is still a matter of debate.[7,8] One of the intriguing features of this material, and other stereoregular materials, is the ability to form transparent gels at sufficiently high supercoolings, as demonstrated by Keller and co-workers for iPS/decalin systems.[9] In the case of sPS, however, various conformations in the crystalline state have been reported and confirmed.[10−12] SPS can crystallize in four crystalline modifications, as shown in Table 1. In the α- and β-modifications, the chains adopt a T_4 all-trans zigzag conformation. These modifications can be subdivided into α', α'', β', and β''.[11−14] In the γ- and δ-modifications, the chains adopt a T_2G_2 helical conformation, where the δ-phase is considered to be a solvent-included phase and the γ-phase a solvent-free phase. The helical modification can only be prepared in the presence of a solvent. It was recognized by Guenet[15] that the occurrence of an invariant liquid−solid line, independent of polymer concentration, in the temperature−concentration phase diagram is indicative for the formation of a polymer/solvent compound. Structure formation takes place on cooling and almost transparent, thermoreversible gels

S0024-9297(97)01292-8 CCC: $15.00
Published on Web 04/08/1998

are formed at relatively low polymer concentrations, similar to iPS.[16] The helical conformation is the structural element in thermoreversible gels, and its formation is largely controlled by kinetic factors.[17,18]

The present paper aims at a detailed study of the phase behavior of sPS with solvents. The phase behavior with *o*-xylene and *cis*-decalin was investigated by Berghmans and co-workers.[17,18] These studies were performed by differential scanning calorimetry (DSC); thus only insight in the thermal effects during the phase transformations was obtained. Further, preliminary in situ X-ray scattering experiments were performed on these systems for a few concentrations.[19] To have a detailed insight into the structural changes during the phase transitions, simultaneous small- and wide-angle X-ray scattering (SAXS and WAXS) and Raman spectroscopy experiments were performed. While SAXS and WAXS can give insight into the morphological changes occurring in the long- and small-range order, the conformational changes occurring during the phase transformations can be followed by Raman spectroscopy. To study molecular conformations in glasses and gels of sPS, vibrational spectroscopic techniques have been used successfully in the past.[20−22]

From the work by Berghmans and co-workers[17,18,23] and by Guenet and co-workers[15,24] some guidelines can be extracted for choosing reactive solvents for sPS. The results on *o*-xylene indicate that the presence of a phenyl ring is favorable to induce a considerable melting temperature depression, which is of importance given the high melting temperature of the pure polymer. This was also illustrated in a paper by Daniel et al. on the thermoreversible gelation of sPS in benzene.[24] A drawback of the solvents *o*-xylene and styrene is their low boiling point, which also makes a detailed analysis of the phase behavior difficult. This drawback can be, to some extent, circumvented by substituting some hydrogen atoms of the phenyl ring by more heavy atoms. The influence of this substitution was systematically studied for a series of chlorobenzenes by Roels et al.[23]

A reactive solvent for sPS should be based on a (substituted) phenyl ring with a polymerizable moiety attached to it. The first choice of course is monomeric styrene. Besides its low boiling point, the major drawback of styrene is that, after in situ polymerization, atactic polystyrene is formed, thus lowering the overall crystallinity of the bulk, and making the resultant material more brittle. Other possible candidates are (meth)acrylates having a phenyl ring, given their high boiling points. In this paper, results on the phase behavior of sPS and two methacrylates will be given, i.e., benzyl methacrylate (BzMA) and cyclohexyl methacrylate (CHMA). These two monomers were chosen as a model system to show the influence of the interaction between the phenyl rings of the solvent and the polymer. The phase behavior has been investigated by DSC and in situ X-ray scattering (SAXS and WAXS) experiments combined with Raman spectroscopy.

II. Experimental Section

A. Materials and Solution Preparation. Syndiotactic polystyrene (sPS) (M_w = 400k) was supplied by DOW Chemical, The Netherlands, and used as received. *cis*-Decalin (Merck) was used as standard solvent, while cyclohexyl methacrylate and benzyl methacrylate, both purchased from Aldrich, were used as reactive solvents. All (reactive) solvents were used without purification. The structural formulas of the used solvents are shown in Figure 1.

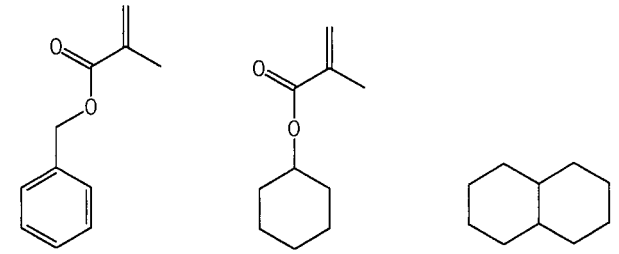

Figure 1. Structural formulas of (A) benzyl methacrylate, (B) cyclohexyl methacrylate, and (C) decalin.

Solutions of sPS were prepared in closed test tubes by dissolving the polymer near the boiling point of the solvent. The solutions were then transferred into disposable pipets, which were quenched in liquid nitrogen. Subsequently, the gels obtained were transferred into Lindemann capillaries for the in situ X-ray and Raman spectroscopy experiments. For studying the phase behavior of sPS and the reactive solvents a sufficient amount of inhibitor (benzoquinone, Aldrich) was added to prevent premature polymerization.

B. Characterization Techniques. B.1. Differential Scanning Calorimetry (DSC). For the study of the phase behavior, sPS powder and solvent (in total ∼20 mg) were sealed in stainless steel pans with rubber O-rings. To construct the phase diagram, calorimetric observations were performed on a Perkin-Elmer DSC-7 apparatus. First, the samples were heated to elevated temperatures in order to dissolve the sPS. Next, the samples were quenched to −20 °C, resulting in gel formation. To measure the phase transformations upon heating quenched sPS/solvent (gels) samples, a constant heating rate of 5 °C/min was employed.

B.2. Simultaneous Small-Angle, Wide-Angle X-ray Scattering (SAXS/WAXS) and Raman Spectroscopy. To follow in situ the morphological and structural changes during the phase transformations in the sPS gels, simultaneous time-resolved small- and wide-angle X-ray scattering (SAXS and WAXS) in combination with Raman spectroscopy experiments were performed on Beamline 8.2 on the Synchrotron Radiation Source (SRS) at the CLRC Daresbury Laboratory, Warrington, U.K. Details of the storage ring, radiation, camera geometry, and data collection system are described elsewhere.[25]

The WAXS data were collected with a curved Inel detector positioned such that its center of curvature coincided with the sample position. The SAXS patterns were collected on a multiwire quadrant detector positioned at 3.5 m from the sample. The SAXS and WAXS data were collected simultaneously in time frames of 36 s. However, due to the low signal-to-noise ratio of the Inel detector, which made the identification of the several modifications difficult, separate time-resolved WAXS experiments were performed on station ID11/BL2 of the European Synchrotron Radiation Facility (ESRF) in Grenoble, France. This beamline can generate a flux of $>10^{12}$ photons/s at the sample position (beam size at the sample is 0.2×0.2 mm^2), compared to the SRS in Daresbury, that generates a flux of 4×10^{10} photons/s at the sample position (beam size at the sample is 0.5×3.5 mm^2). The beam is tunable in the energy range 7−100 keV; a wavelength of 0.757 Å was used throughout the experiments. Detection of the scattered photons was established with a Princeton CCD detector.

For calibration of the SAXS detector, the scattering pattern from an oriented specimen of wet collagen (rat-tail tendon) was used. PE single crystals were used to calibrate the WAXS detector. A parallel plate ionization detector was placed in front of the sample to record the incident intensity to correct for changes of the beam intensity.

The conformational changes were simultaneously investigated by Raman spectroscopy. Raman spectra were recorded with a Kaiser Optical Systems "Holoprobe 532" in time frames of 36 s. The Raman spectrometer is contained in a transport-

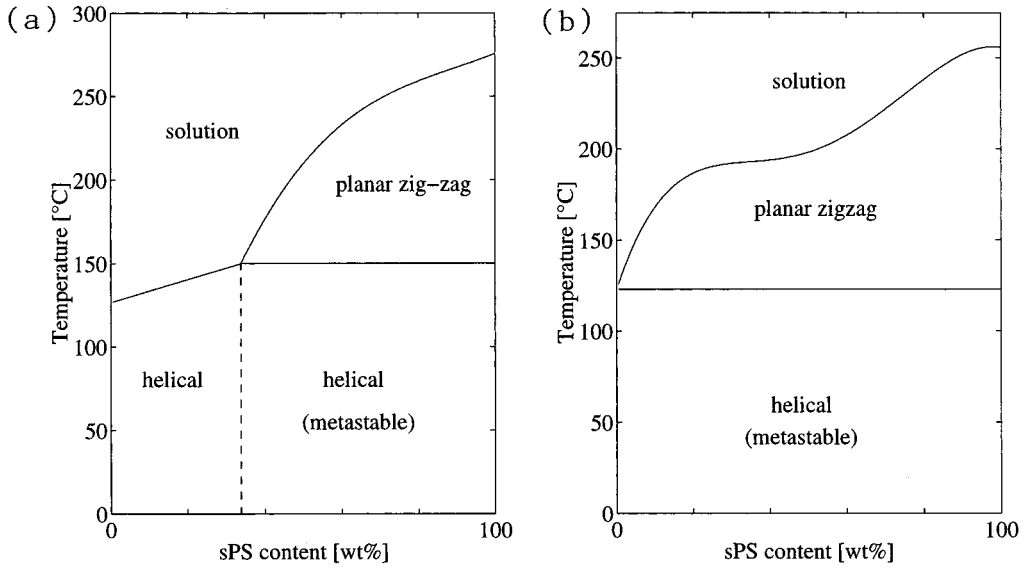

Figure 2. Schematic temperature−composition phase diagrams for syndiotactic polystyrene (sPS) and solvents: (a) sPS/good solvent; (b) sPS/poor solvent.

able box, comprising a frequency-doubled, diode-pumped Nd:YAG laser source with an excitation line of 532 nm, a holographic filter to reject the unshifted laser light, a *f*/1.8 aberration-corrected imaging spectrograph, and a thermoelectrically cooled CCD detector. Essential for the combined SAXS/WAXS/Raman spectroscopy experiments is that remote sampling could be carried out with a fiber-optic probe, with one fiber to deliver the laser light and the other one to collect the scattered light through a confocal sample head. Details of this sample head are described in a paper by Everall et al.[26] The probe head was screwed on a flexible arm, fixed on a XYZ translator for positioning, and controlled imaging of the light using a 10× objective onto the sample. In this way, the Raman spectra were obtained in the backscattering mode. Further details of the SAXS/WAXS/Raman spectroscopy measurements are given in a paper by Bryant et al.[27]

Quenched sPS gels with known composition were transferred into Lindemann capillaries and, subsequently, sealed (see previous section). The capillaries were placed in a capillary holder, fixed on a Linkam THMS 600 heating−cooling stage, of which the position could be controlled via an XYZ stage. The silver heating block of the hot stage contained a 4 × 1 mm^2 conical hole allowing the X-rays to pass through unhindered. The hot stage was controlled with a TMS-92 controller and a Linkam LN2 cooling unit, enabling cooling rates up to 130 °C/min, necessary for quenching. A heating and cooling rate of 5 °C/min was used during the phase transformation studies, similar to the DSC scans.

III. Phase Behavior of SPS and Standard Solvents: A Brief Recapitulation of Literature Data

To understand the influence of the solvent quality on the thermodynamic stability of various modifications of sPS, we summarize the state of the art of this subject in this section as a starting point for the experimental work performed in this paper.

Phase Behavior of sPS/Good Solvent (*o*-Xylene) and sPS/Poor Solvent (*cis*-Decalin). In the case of sPS, it has been stated that sPS can form compounds with specific solvents. Compound formation will change the phase diagram; a maximum in the temperature−concentration diagram will be anticipated at the composition of this compound, of which the melting temperature corresponds to the congruent melting temperature of the compound.[15,28] The situation becomes different when the compound decomposes before melting, and incongruent melting will be observed. This latter situation is more realistic for sPS−solvent systems, since decomposition of the compound before melting has been observed for several solvents.

The general phase diagrams as shown in Figure 5 of ref 28 describe the phase behavior for different polymer/solvent systems under equilibrium conditions. Nevertheless, the majority of observations on real systems, measured under nonequilibrium conditions, can be interpreted using these general phase diagrams. The experimentally determined phase diagrams of sPS and two solvents of different quality, i.e., *o*-xylene (a good solvent) and *cis*-decalin (a poor solvent), were investigated by Berghmans and co-workers.[17,18] The schematic phase diagrams for sPS and a good solvent and for sPS and a poor solvent are given in Figure 2a,b, respectively.

In the case of a good solvent, Figure 2a, the crystalline α- or β-phase (planar zigzag conformation) is thermodynamically the stable phase at high polymer concentrations, while at lower concentrations, the compound (helical δ-phase) is thermodynamically the stable phase. When concentrated solutions are quenched, the (metastable) helical δ-phase is observed. The borderline (dashed vertical line in Figure 2a) between the stable and metastable helical phase is unknown and estimated to be at 40 wt % sPS in the case of sPS/*o*-xylene by Berghmans.[17] In the case of a poor solvent, for example, decalin, the α- or β-phase (planar zigzag conformation) is the stable phase over the whole concentration range (see Figure 2b). Due to the poor solvent quality, the melting point depression, L−S, is less than in the case of a good solvent. The occurrence of a plateau in the L−S curve, Figure 2b, is usually related to the occurrence of liquid−liquid (L−L) demixing (UCST) interfering with the liquid−solid (L−S) curve, viz. the melting point depression curve. However, in the case of sPS/decalin systems, the L−L demixing region is located far below the melting temperature depression curve and the observed plateau cannot be a result of interference of L−L demixing with crystallization (L−S). The plateau region was explained by Berghmans and co-workers by compound formation.[23]

The nonequilibrium character of the measurements used to construct the phase diagram reveals the influ-

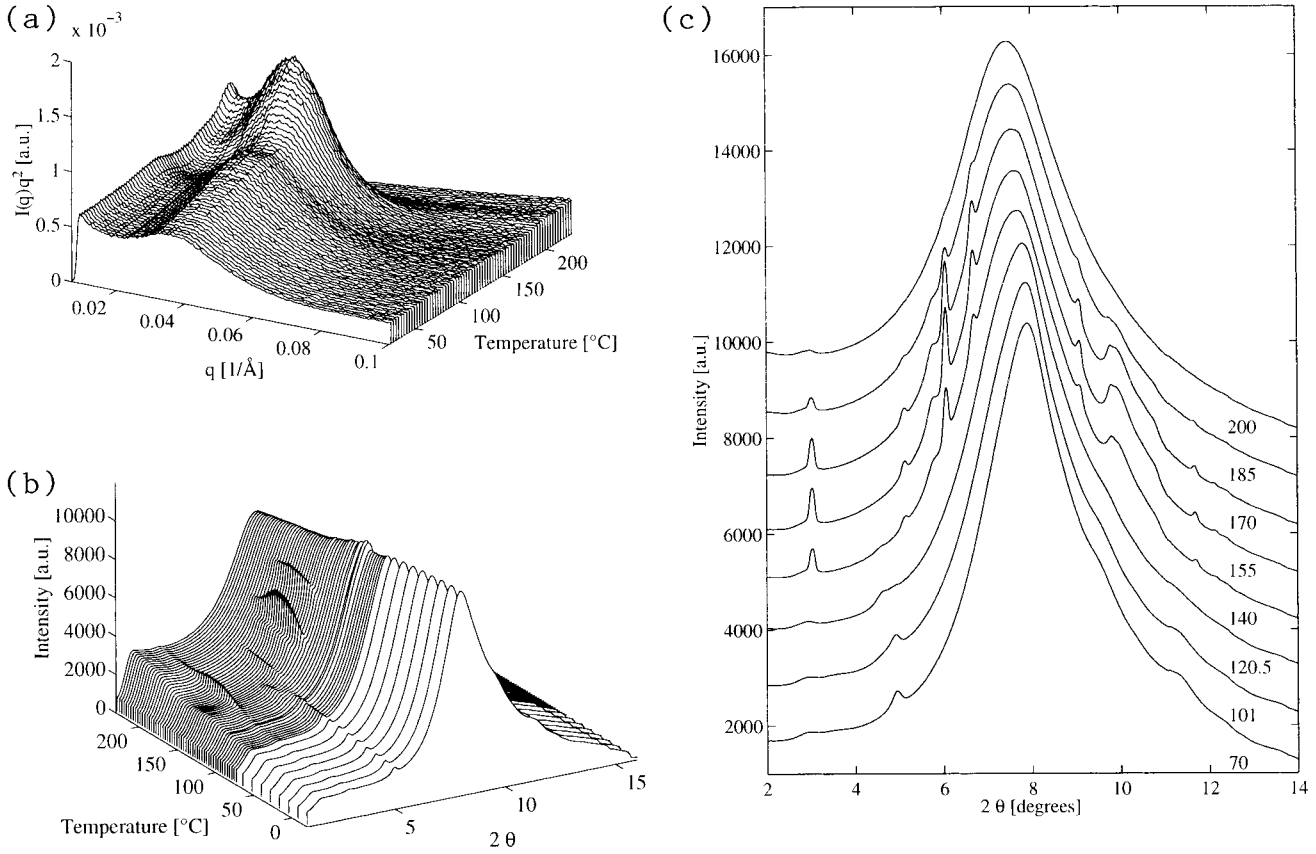

Figure 3. Heating run of a quenched 20 wt % sPS/decalin sample: (a) 3-D plot of SAXS data, heated from 20 to 230 °C at 5 °C/min; (b) 3-D plot of WAXS data, heated from −20 to 70 °C at 10 °C/min and from 70 to 230 °C at 2.5 °C/min; (c) 2-D plot of WAXS data (temperatures are indicated in the plot).

ence of the kinetics on the phase transitions. Though the α- or β- (planar zigzag) phase is the most stable phase for sPS in decalin, the compound is obtained upon quenching. The relative amount of the different phases, α or β vs δ, is dependent on the cooling rate. Upon slow cooling, the stable α- or β-phase is formed, whereas at a high cooling rate, compound formation is promoted. This implies that the compound is metastable over the entire concentration range in the case of poor solvents. In the case of a good solvent, a stable helical δ-phase is obtained at lower concentrations.

IV. Results

A. Phase Behavior of sPS and Decalin. Small- and Wide-Angle X-ray Scattering (SAXS and WAXS) of sPS/Decalin Systems. Earlier observations on the phase behavior of sPS in *cis*-decalin[17] and *o*-xylene[18] were mainly based on thermal analysis. Some additional information on the phase behavior was given by X-ray experiments.[17,18] This latter technique was mainly used to show the structural differences between the helical and the planar zigzag conformation. However, the experimental observations were not conclusive in the distinction of particular phases at specific temperatures. In the next paragraphs, more evidence, based on in situ X-ray scattering experiments, will be presented as an extension of the earlier DSC observations and a more quantitative interpretation of the phase diagram of sPS/decalin. Recently, a preliminary in situ X-ray and FTIR study has been performed by Roels et al. on the 40 wt % sPS/*cis*-decalin system.[19]

In Figure 3 the results of the in situ X-ray scattering experiments are depicted for the 20 wt % sPS/decalin system. The SAXS and WAXS data were collected upon heating the sPS/decalin gels. The SAXS data are shown in Figure 3a as a 3-D plot of the Lorentz-corrected intensity, $I(q)q^2$, versus the scattering vector, $q = (4\pi/\lambda) \sin \theta$, where 2θ is the scattering angle, and temperature. The WAXS data are shown in Figure 3b as a 3-D plot of intensity, $I(2\theta)$, versus scattering angle 2θ and temperature. Since this 3-D plot gives only a general impression of the structural changes taking place on heating, representative 2-D plots of the WAXS data, collected at the indicated temperatures, are shown in Figure 3c in order to identify the crystal structure.

Table 2. Diffraction Angles (deg) and Bragg Distances (Å) Observed in the WAXS Spectra for the 20 wt % sPS/Decalin System at −20 °C

hkl	d_{obs}	$2\theta_{obs}$	*hkl*	d_{obs}	$2\theta_{obs}$
200	8.71	4.98	200	3.83	11.32
	4.53	9.59		3.52	12.33

The wide-angle X-ray diffraction pattern at the start of the heating run is characterized by a broad halo from the solvent centered around $2\theta = 8.0°$ and less intense reflections at 2θ = 5.0, 9.6, 11.3, and 12.3°. The corresponding *d* values are given in Table 2. These reflections match with the known helical structure for the δ-phase. This phase is stable up to a temperature of approximately 100 °C. At higher temperatures, the intensity of the 2θ = 5.0° reflection (d = 8.71 Å) diminishes and at the same time a small peak is observed at a slightly lower angle (see Figure 3c, T = 120.5 °C). This is indicative for a different helical phase. The nature of this helical phase will be discussed in section V.A. On continued heating, a transformation

Table 3. Diffraction Angles (deg) and Bragg Distances (Å) Observed in the WAXS Patterns of sPS in Decalin Compared with the Bragg Distances for the β''-Phase As Observed by Guerra[12] and Calculated by Chatani et al.[11]

hkl	$d_{Chatani}$	d_{Guerra}	d_{obs}	$2\theta_{obs}$
020	14.40	14.34	14.32	3.03
110	8.425	8.48	8.47	5.12
120	7.516	7.52	7.48	5.77
040	7.205	7.17	7.16	6.06
130	6.493	6.49	6.50	6.68
060	4.803	4.78	4.78	9.09
111	4.338	4.38	4.37	9.93
170	3.730	3.72	3.73	11.66

into the planar zigzag conformation at approximately 150 °C occurs and finally melting takes place. A comparison of the *d* values with the earlier reported results from Guerra et al.[12] and Chatani et al.[11] shows that this planar zigzag conformation corresponds to the β''-phase (see Table 3).

The structural changes occurring on heating also influence the morphology as can be seen from the SAXS results in Figure 3a. The broad maximum initially present at $q = 0.04$ Å^{-1} ($d = 157$ Å) is indicative for the presence of long-range order. The intensity of this maximum increases during the helical to helical transformation at around 120 °C, simultaneously with the observed changes by WAXS. The transformation into the planar zigzag conformation at approximately 150 °C has a more dramatic influence on the morphology. This is observed first as a decrease in intensity followed by an increase and a simultaneous shift of the maximum from $q = 0.04$ to 0.03 Å^{-1} ($d = 209$ Å). Once the transformation into the β-phase occurs, a lamellar morphology will set in, as earlier investigated by transmission electron microscopy.[29] The resultant maximum in the SAXS pattern corresponds to the average lamellar thickness. The shift in the SAXS maximum to lower angles on further heating corresponds to the anticipated increase in the lamellar thickness. Continued heating results in a drop in intensity due to melting of the lamellae.

In Figure 4, the WAXS and SAXS data are shown for 40% sPS/decalin. According to Berghmans and coworkers, the concentration dependence on the phase behavior of sPS and decalin is most conspicuous around a polymer concentration of 40 wt %, as shown in Figure 1 of ref 17. In this paper, it was suggested that at 40 wt % sPS almost all solvent molecules may participate in the compound formation of the helical δ-phase. From the WAXS results of the 40 wt % sPS/decalin system, as shown in Figure 4, it is evident that at the very initial stage of the heating scan, the δ-phase is present. However, the reflections at $2\theta = 3.03°$ and 6.1° show that part of the sPS molecules have crystallized into the β-phase. The structural and morphological changes during the heating run are similar to the changes observed for the 20 wt % system, except that the transition from the helical to the β-phase, as observed by SAXS, is more prominent and that the melting temperature of the β-phase is higher, as anticipated from the phase diagram.[17] The results presented above, concerning the structural and morphological changes during heating, support to a large extent the DSC observations of Berghmans and co-workers.[17,18]

B. Phase Behavior of sPS and Benzyl Methacrylate. Consecutively, the DSC results from the 20 and 40 wt % sPS/BzMA systems and the results of the combined SAXS and WAXS experiments on the 40 wt % system will be given. This is followed by the simultaneously obtained Raman results of the same system. This section is concluded by SAXS/WAXS data of the 20 wt % sPS system.

Differential Scanning Calorimetry. In Figure 5a,b the DSC results of a heating scan of two concentrations, 20 and 40 wt % sPS, respectively, are depicted. Before assigning the endo- and exotherms, it is important to describe the thermal history. The samples in the sealed DSC pans were heated to above the melting temperature and left for some minutes to homogenize. The samples were, subsequently, quenched to −20 °C, before the actual measurements were performed.

For the 20 wt % sPS sample, three large endotherms with peak temperatures of 115, 160, and 180 °C together with one exotherm at 130 °C are observed. The first, broad endotherm represents the melting of the helical phase. This is followed by the exotherm, which represents the crystallization into the planar zigzag phase. The two high-temperature endotherms correspond to melting of crystals with two lamellar thicknesses or melting and recrystallization of the planar zigzag phase.

Three endotherms and one exotherm are also observed for the 40 wt % sPS system. The position of the first endotherm is at the same temperature as that for 20 wt % sPS. This is similar to the observations made by Guenet[15] and later by Deberdt and Berghmans[17] that the melting temperature of the helical phase is independent of the polymer concentration. It is also observed that the melting temperature of the planar zigzag phase increases with polymer concentration. Furthermore, the second endotherm of the planar zigzag phase is much larger, which may be a result of the formation of thicker and less defected crystals in the planar zigzag phase than for the 20 wt % sPS system.

Small- and Wide-Angle X-ray Scattering (SAXS and WAXS) of the 40 wt % sPS System. The results of the SAXS and WAXS experiments obtained during the heating scan of the 40 wt % sPS/BzMA system are depicted in Figure 6. Similar to the 40 wt % sPS/decalin system (see section IV.A), the sPS chains have adopted a helical conformation in the quenched material. The quenched sample shows the existence of the δ-phase at −20 °C. This is characterized by rather sharp reflections at $2\theta = 2.9$, 5.1, 9.7, 11.1, 11.6, 12.3, and 13.7°. The corresponding *d* values are shown in Table 4. The existence of the δ-phase implies that benzyl methacrylate can form a molecular compound with sPS. The weak reflections at $2\theta = 6.1$ ($d = 7.08$ Å) and 6.8° ($d = 6.41$ Å) are from the β-phase, which seems to have been formed during quenching, similar to the 40 wt % sPS/decalin system (see Figure 4). These crystals formed in the β-phase are stable even at higher temperatures. At approximately 50 °C, two broad reflections centered around $2\theta = 3.6$ ($d = 12.05$ Å) and 8.8° ($d = 4.91$ Å) appear simultaneously. These reflections are much more pronounced in the 20 wt % sPS/BzMA system, as will be shown in Figure 8. Similar reflections are also observed for the sPS/CHMA systems, which will be discussed in section IV.C. However, these reflections were not present in the sPS/decalin systems. On continued heating, the reflection at $2\theta = 3.6°$ disappears and the reflection at $2\theta = 8.8°$ shifts to higher angles, while a sharp reflection around $2\theta = 8.0°$ appears. Simultaneously, the reflection at $2\theta = 5.1°$ gradually shifts to lower angles and the sharpness of this reflection decreases. These changes are related to transfor-

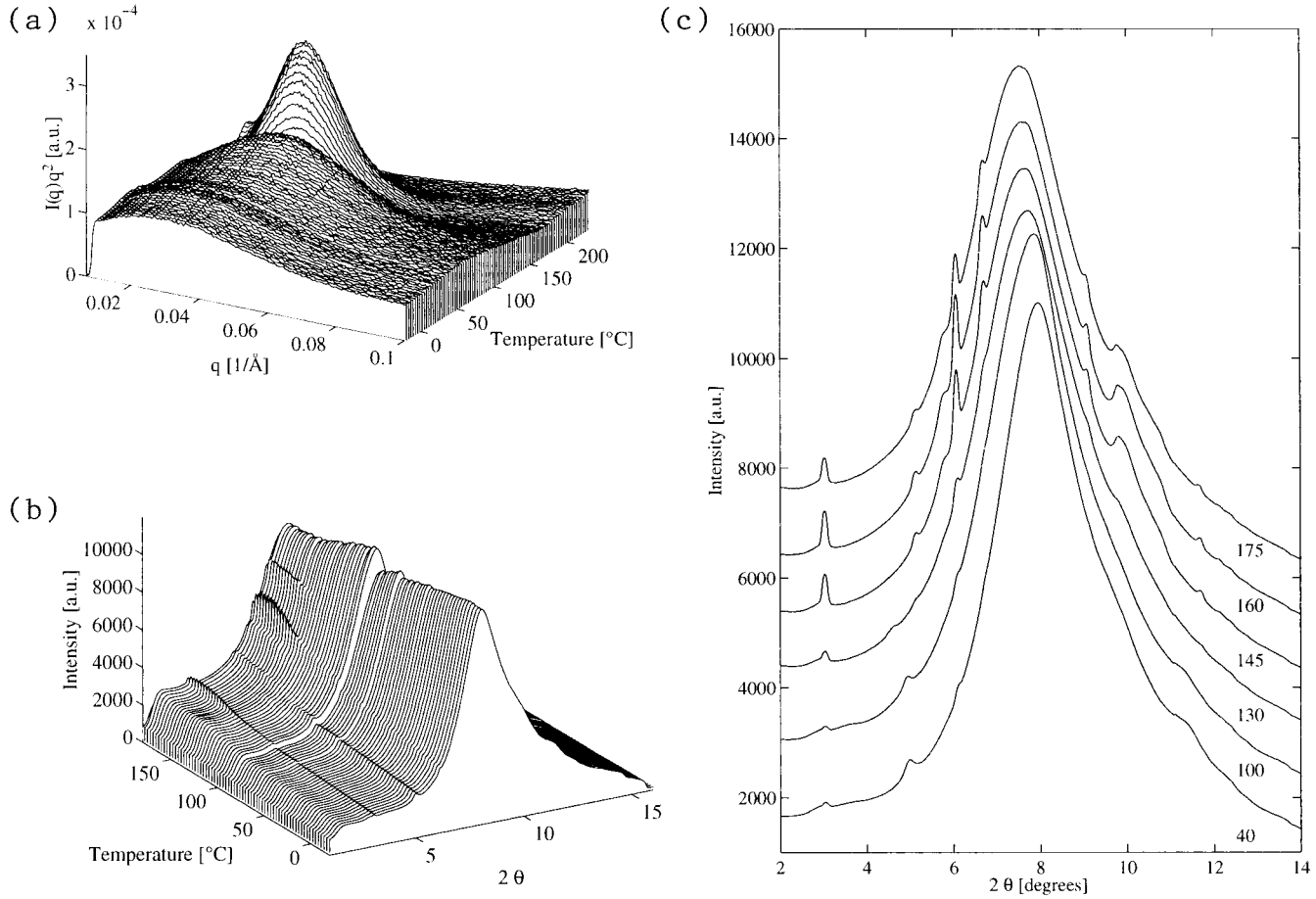

Figure 4. Heating run from −20 to +230 °C at 5 °C/min of a quenched 40 wt % sPS/decalin sample: (a) 3-D plot of SAXS data; (b) 3-D plot of WAXS data; (c) 2-D plot of WAXS data (temperatures are indicated in the plot).

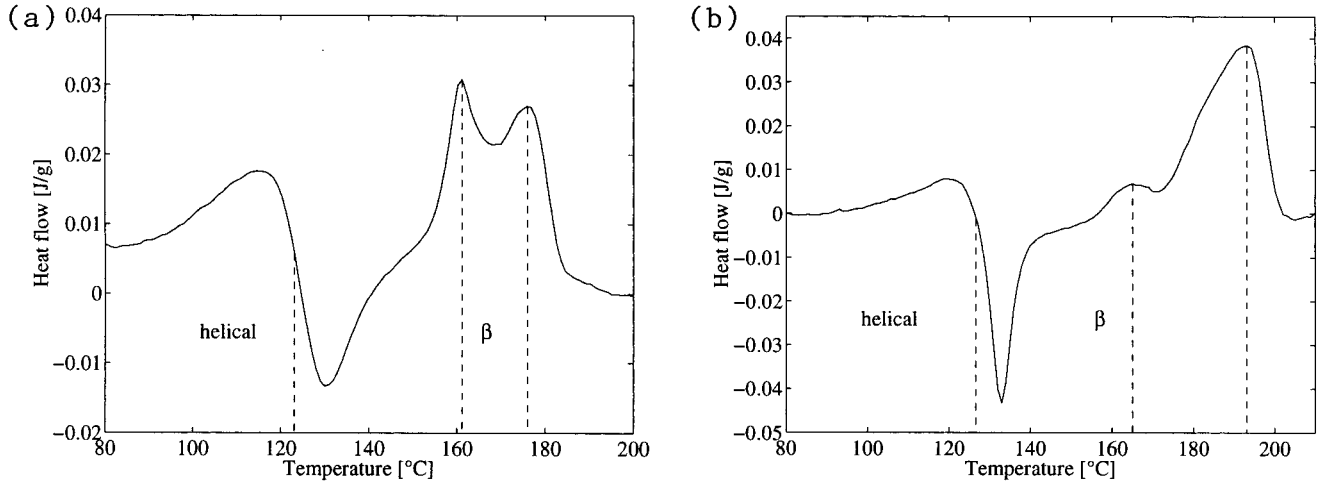

Figure 5. DSC traces of sPS/BzMA systems: (a) 20 and (b) 40 wt % sPS.

mations within the helical δ-phase. The nature of the thus newly formed helical phase will be discussed in section V.A. On heating beyond a temperature of 130 °C, we observe that the reflections corresponding to the helical phase disappear with a subsequent incoming of sharp reflections associated with the crystalline β-phase. Similar to the sPS/decalin systems, the exact d values of this β-phase match the earlier defined β''-phase.[12] See also Table 3 for the d values of this phase.

In the quenched sample, no distinct maximum in the SAXS pattern is observed (see Figure 6a). The absence of a maximum prevails up to a temperature of approximately 100 °C. Above this temperature, as the structural changes in the helical phase (as observed by WAXS) set in, a broad maximum at $q = 0.05$ Å^{-1} (d = 126 Å) appears, which intensifies and shifts to lower angles up to a temperature of 130 °C. On the helical to β transition, the SAXS data show that the maximum decreases in intensity. On subsequent heating, the incoming of a strong maximum at $q = 0.03$ Å^{-1} (d = 209 Å) is indicative for the formation of the anticipated lamellar morphology in the β-phase. The continued heating leads to a shift of the maximum to lower q values, indicating the expected increase in the lamellar

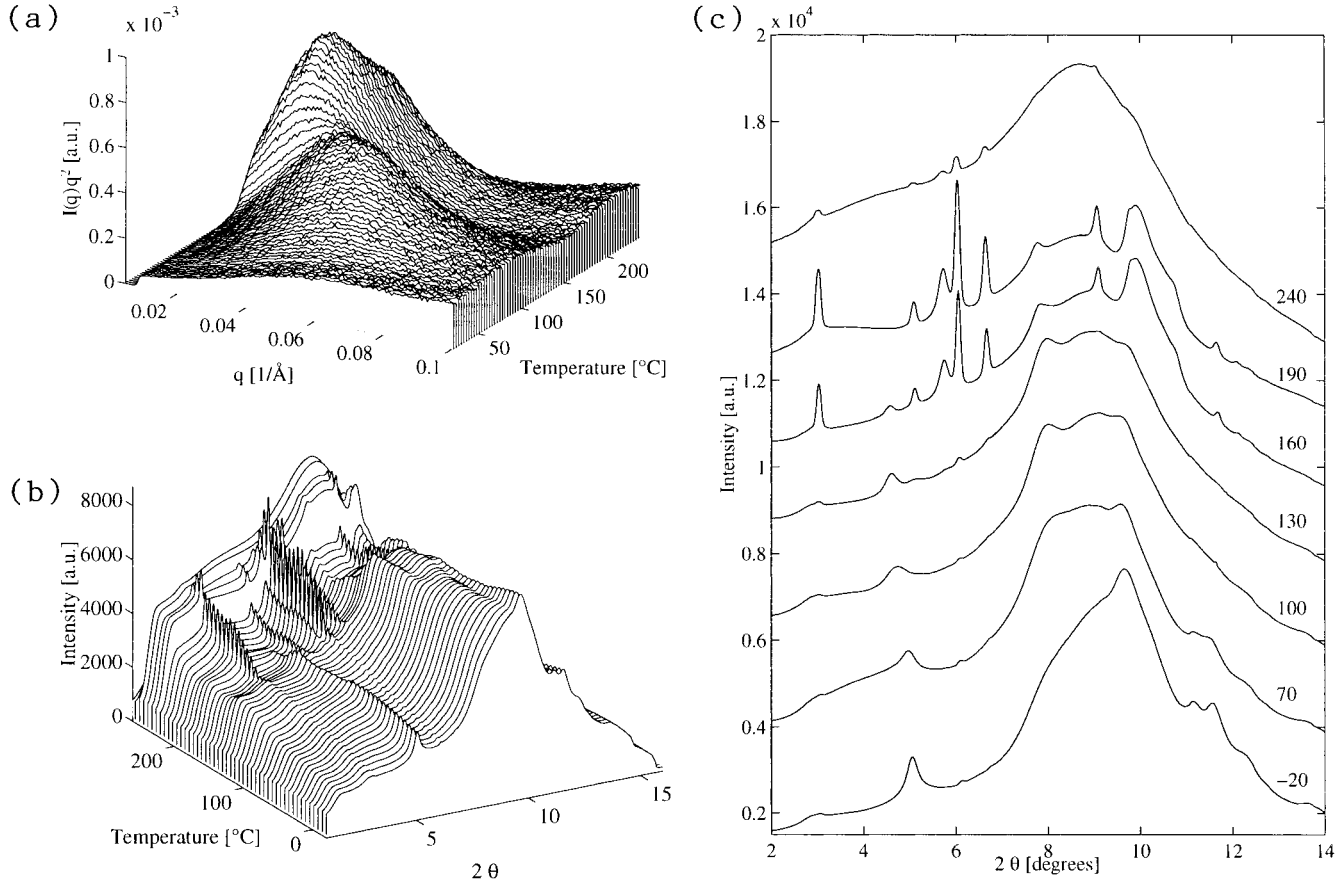

Figure 6. Heating run of a quenched 40 wt % sPS/BzMA sample: (a) 3-D plot of SAXS data from 20 to 230 °C at 5 °C/min; (b) 3-D plot of WAXS data from −20 to 230 °C at 5 °C/min; (c) 2-D plot of WAXS data (temperatures are indicated in the plot).

Table 4. Diffraction Angles (deg) and Bragg Distances (Å) Observed in the WAXS Spectra for the 40 wt % sPS/BzMA System at −20 °C

hkl	d_{obs}	$2\theta_{obs}$	*hkl*	d_{obs}	$2\theta_{obs}$
010	15.17	2.86	200	3.76	11.57
200	8.59	5.05		3.54	12.27
	4.50	9.66		3.18	13.67
	3.90	11.14			

thickness at higher temperatures before melting.

Raman Spectroscopy of the 40 wt % sPS System. Besides morphological and structural changes studied by SAXS and WAXS, changes in the polymer conformation will occur upon heating. The conformational changes were simultaneously followed by Raman spectroscopy and the results of the heating run of a quenched 40 wt % sPS/BzMA system are shown in Figure 7. To show the overall changes as a function of temperature, the Raman spectra are shown as a 3-D plot of the intensity versus wavenumber and temperature in Figure 7a.

Since the Raman spectra were recorded in the backscattering mode, changes in the overall intensity provide information about variations in the scattering power due to the phase transitions. The amount of the Raman radiation collected on the spectrometer will depend on two factors: (a) the volume exposed by the incident light, which would be more for transparent samples; (b) the Raman events per unit volume, which would be more in a diffusely scattering sample. Overall changes in the backscattered intensity will be a balance between these two factors. In our case, it appears that factor a, i.e., the volume exposed to the incident light, seems to have the upper hand.

The intensity of the peak at approximately 1000 cm^{-1}, which originates from the breathing mode vibration of the phenyl ring and should not change in intensity, can be considered as an internal calibration for the backscattered intensity. On heating, the intensity is almost constant up to a temperature of approximately 90 °C (this is marked as 1 in Figure 7a). The changes occurring between 90 and 100 °C (2) are due to the helical to helical transformation, as observed simultaneously by WAXS. This is followed by an increase and decrease of the intensity in the temperature region of 100−150 °C (3). The increase is due to melting of the helical phase, while the decrease is related to crystallization into the β-phase, as observed by SAXS/WAXS. The further increase of the intensity beyond 170 °C (4) is a result of melting of small crystals of the β-phase. This is in line with the endotherm at 165 °C in the DSC trace, as shown in Figure 5.

A number of vibrational spectroscopy studies have been carried out on the different polymorphs and transformations in sPS.[20−22,30] A characteristic peak at 1222 cm^{-1} has been assigned to the presence of an all-trans conformation and was used to estimate the degree of crystallinity[31] and crystallization rate.[32] Kobayashi et al.[30] used Raman and infrared spectroscopy to study the differences between the helical and planar zigzag forms. Differences were found in the 700−800 cm^{-1} region, in which the phenyl ring vibration modes have been shown to manifest themselves through the presence of two peaks resulting from conformational changes in the alkyl backbone. For the planar zigzag conformation, a strong, sharp peak at 770 cm^{-1} with a broad peak at approximately 795 cm^{-1} was attributed to the all-

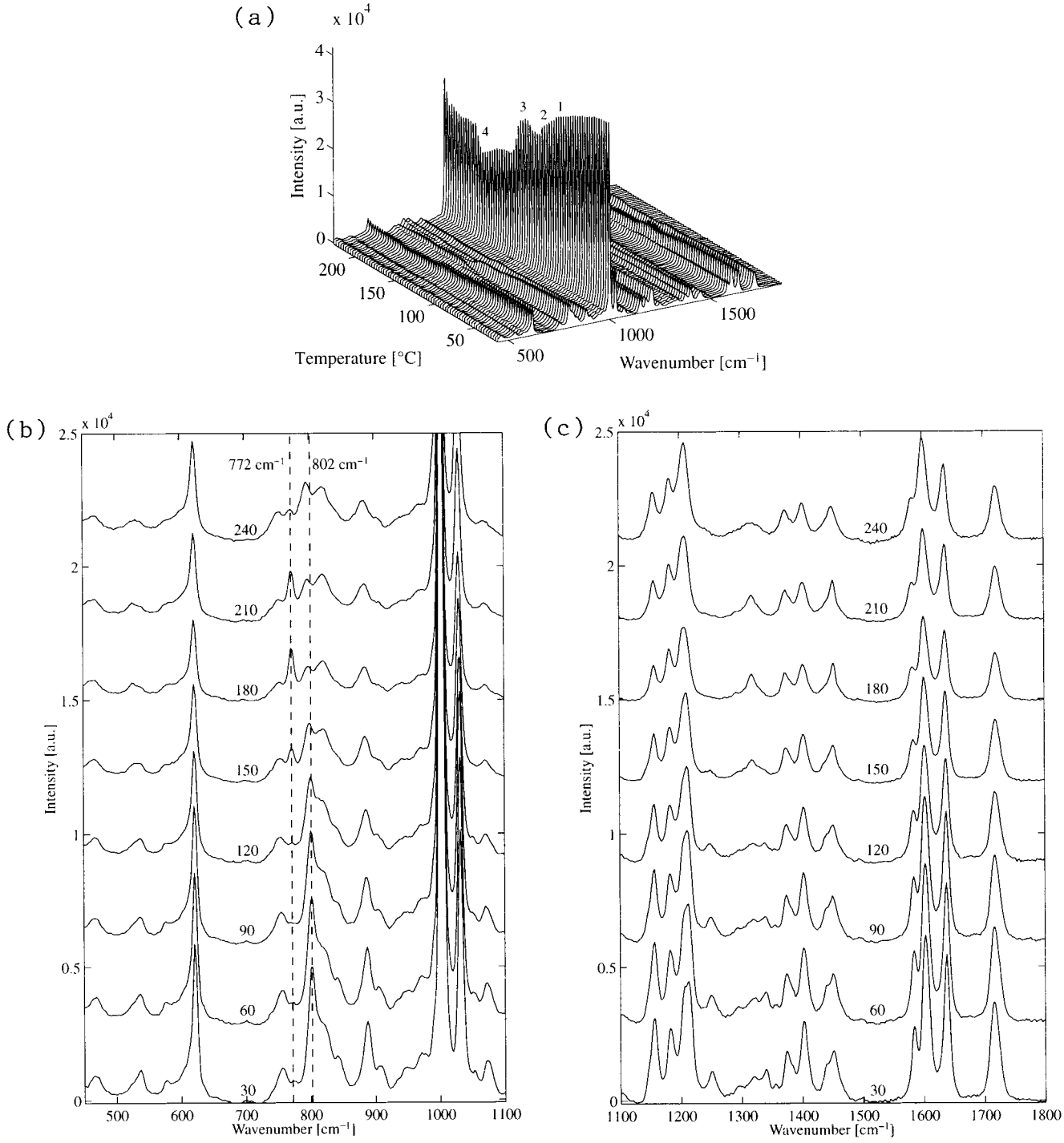

Figure 7. Heating run from 20 to 230 °C at 5 °C/min of a quenched 40 wt % sPS/BzMA sample: (a) 3-D plot of Raman data; (b) 2-D plot of region 450−1100 cm^{-1}; (c) 2-D plot of region 1100−1800 cm^{-1}. Temperatures are indicated in plots b and c. Markers 1−4 i (a) indicate temperatures of 90, 100, 150, and 170 °C, respectively.

trans conformation. The strong peak at 798 cm^{-1} was assigned to the helical phase. The weak peak at 769 cm^{-1} was associated to the mixed trans−gauche conformation. These assignments will be used to follow the phase transitions in our studies, as reported below.

For a more detailed analysis on the conformational changes, representative 2-D plots collected at the indicated temperatures are shown for the spectral regions 450−1100 and 1100−1800 cm^{-1} in Figure 7b,c, respectively. From the strong peak at 802 cm^{-1} at the starting temperature, it is evident that the chains have adopted the helical conformation in the presence of BzMA. On heating, this peak vanishes above a temperature of approximately 130 °C and a new peak at 772 cm^{-1} appears, which indicates the incoming of the all-trans planar zigzag conformation. This peak almost disappears at the melting temperature of the all-trans planar zigzag phase, 240 °C. The changes in the helical phase are not easy to distinguish. Only a small decrease in the intensity of the 802 cm^{-1} peak is observed. This was also found in the study from Kellar et al.,[22] who showed that there is virtually no difference between the δ- and the γ-polymorphs within the 700−800 cm^{-1} region.

Small- and Wide-Angle X-ray Scattering (SAXS and WAXS) of the 20 wt % sPS System. The SAXS

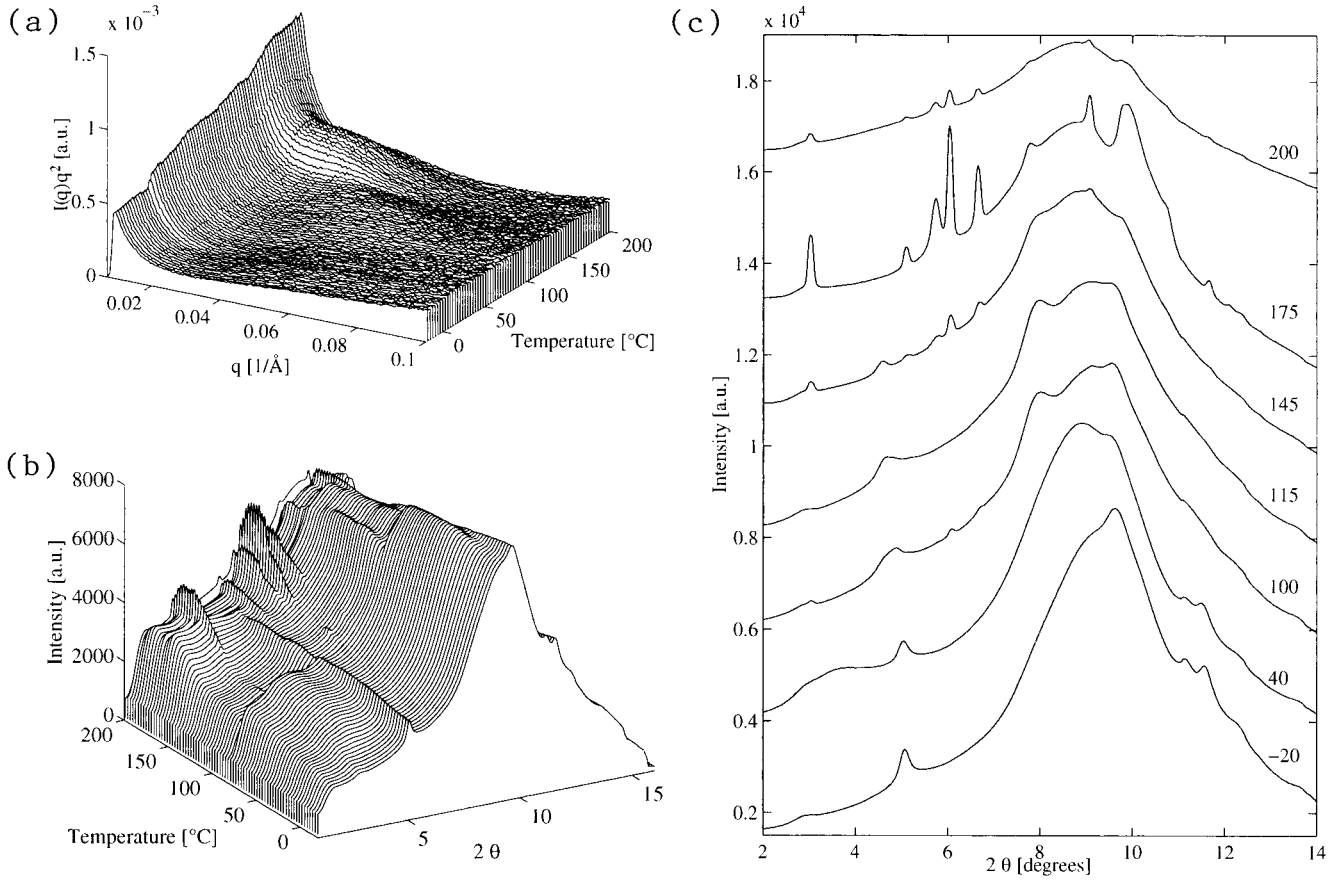

Figure 8. Heating run from −20 to +230 °C at 5 °C/min of a quenched 20 wt % sPS/BzMA sample: (a) 3-D plot of SAXS data; (b) 3-D plot of WAXS data; (c) 2-D plot of WAXS data (temperatures are indicated in the plot).

and WAXS results of the heating scan of the 20 wt % sPS/BzMA system from −20 to +230 °C at 5 °C/min are shown in Figure 8. A few differences are observed in comparison to the 40 wt % sPS system (Figure 6). First, the SAXS data show that at a temperature of approximately 30 °C a sudden change in the scattered intensity at the lowest observable q values occurs. At the same temperature, the incoming of two broad reflections in the WAXS data centered around $2\theta = 3.6$ ($d = 12.05$ Å) and 8.8° ($d = 4.91$ Å) is observed, which intensify on further heating. These reflections were also present for the 40 wt % system but are much stronger for the 20 wt % system. The reflection at $2\theta = 5.1°$ ($d = 8.59$ Å) is indicative of the presence of the δ-phase at these temperatures. The second observed difference is the absence of crystals in the β-phase in the quenched sample unlike in the 40 wt % system (see Figure 7). On subsequent heating during the (structural) changes in the helical phase, the reflection at $2\theta = 5.1°$ becomes broader, while the reflection centered around $2\theta = 3.6°$ disappear and the reflection at 8.9° shifts to higher angles. These results are in line with the helical to helical transformation, as observed for the 40 wt % sPS/BzMA system (Figure 7). However, small reflections at $2\theta = 6.1$ and 6.7° ($d = 7.16$ and 6.50 Å) associated with the β-phase appear after the transformation, as seen in Figure 8c at 100 °C. From the intensity of these reflections, it is evident that only a small fraction of the polymer has transformed into the β-phase. The incoming of the β-phase is remarkable at these low temperatures and even more surprising is the disappearance of these reflections on further heating (see Figure 8c, $T = 115$ °C). This shows that the β-phase is metastable under these conditions and can coexist with the helical phase at these temperatures and this composition. The metastability of the β-phase crystallized under these conditions will be discussed in section V.B.

Further, on comparison of the SAXS data for the 20 wt % sPS/BzMA (Figure 8a) and 40 wt % sPS/BzMA systems (Figure 6a), it is evident from the intensities that the electron density fluctuations between the polymer and solvent rich domains within the quenched gel are relatively low for the 20 wt % sPS/BzMA system in comparison to the 40 wt % system. This is an indication of the fact that the difference between the polymer concentration in the polymer rich domain and the solvent rich domain is less for the 20 wt % system than for the 40 wt % system.

C. Phase Behavior of sPS and Cyclohexyl Methacrylate. Also for this reactive solvent, in a similar way as in section IV.B, first the DSC results will be given, followed by the SAXS/WAXS data and, finally, the Raman results.

Differential Scanning Calorimetry. The phase behavior of sPS/cyclohexyl methacrylate (CHMA) was investigated by DSC. Figure 9 shows the DSC results of a heating scan of the 40 wt % sPS/CHMA system. The temperature history before starting the actual measurement is identical to the one described in section IV.B.

For the 40 wt % sPS system, three endotherms with peak temperatures of 120, 165, and 195 °C and one sharp exotherm at 130 °C are observed. The position of the first endotherm, which is associated with melting of the helical phase, is at the same temperature as measured for the sPS/BzMA systems. Similar to the sPS/BzMA systems, the melting temperature of the

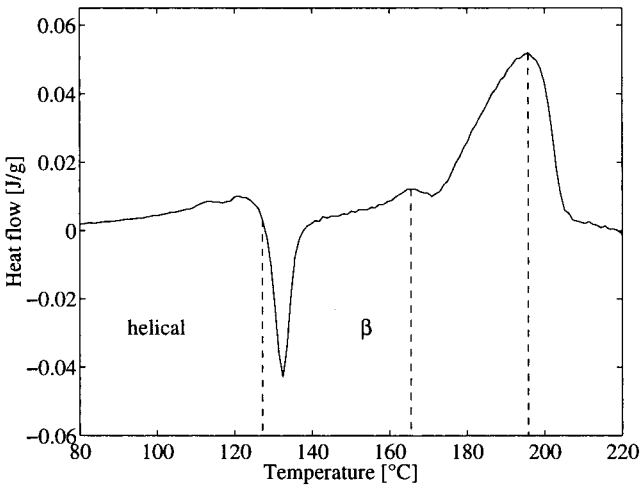

Figure 9. DSC trace of the 40 wt % sPS/CHMA system.

Table 5. Diffraction Angles (Å) and Bragg Distances (deg) Observed in the WAXS Spectra for the 40 wt % sPS/CHMA System −20 °C

hkl	d_{obs}	$2\theta_{obs}$	*hkl*	d_{obs}	$2\theta_{obs}$
010	14.70	2.95	200	3.91	11.12
200	8.87	4.89		3.71	11.71
	5.31	8.19		3.53	12.32
	4.49	9.67		3.19	13.61

helical phase is independent of the polymer concentration. Moreover, the positions of the melting endotherms of the β-phase are at the same temperatures for both solvents.

Small- and Wide-Angle X-ray Scattering (SAXS and WAXS) of the 40 wt % sPS System. The difference observed in the quenched samples of the 40 wt % sPS/BzMA and 40 wt % sPS/CHMA systems is found in the WAXS. Besides the known reflections at 2θ = 2.9, 4.9, 9.7, 11.1, 11.7, 12.3, and 13.6° assigned to the δ-phase (for the corresponding *d* spacings (see Table 5), a strong reflection at $2\theta = 8.2°$ ($d = 5.31$ Å) is observed in the quenched 40 wt % sPS/CHMA system, as shown in Figure 10c at −20 °C. This reflection is characteristic of the presence of the helical phase observed for the sPS/BzMA systems at higher temperatures (see Figure 6c).

The transformation from the helical to the β-phase also displays some differences in the WAXS data, despite the similar DSC and SAXS observations for sPS/CHMA and sPS/BzMA systems. The major difference is the appearance of a broad, strong reflection centered around 2θ = 3.8° above 150 °C, together with the increase in intensity of the broad reflection at $2\theta = 8.0°$ (d = 5.43 Å). The origin of these reflections can only be sought in solvent specific diffractions. This will be discussed in connection with the Raman spectroscopy results, which follow below.

Raman Spectroscopy of the 40 wt % sPS System. The Raman spectroscopy results of the heating run from 20 to 240 °C at 5 °C/min of the 40 wt % sPS/CHMA system are depicted in Figure 11. Figure 11a shows the Raman spectra as a 3-D plot of the intensity versus wavenumber and temperature. Representative 2-D plots collected at the indicated temperatures are shown for the spectral regions 450−1100 and 1100−1800 cm^{-1} in parts b and c, respectively. The position of specific peaks for the helical and planar zigzag conformations were already discussed in section IV.B.

Similar to the intensity variation of the 1000 cm^{-1} peak for the sPS/BzMA system (see Figure 7), the variation in the backscattered intensity of this peak can be used for the sPS/CHMA system to follow the phase transitions. On heating, the intensity is almost constant up to a temperature of 100 °C (marked as 1 in Figure 11a). On heating further, a large increase of the intensity is observed, which accompanies the melting of the helical phase (2), resulting in a transparent solution, and thus an increase of the backscattered intensity. Recrystallization into the β-phase, which would result into an opaque solution, is observed by a sharp decrease in the backscattered Raman intensity (3).

Similar to the sPS/BzMA system, from the presence of a strong peak at 802 cm^{-1}, it is evident that the chains have adopted a helical conformation in the quenched sPS/CHMA system (see Figure 11b). On heating, the intensity of this peak drops considerably above a temperature of approximately 130 °C, leaving only a broad peak centered around 800 cm^{-1}, which is due to the vibrational mode of CHMA. The simultaneous appearance of a new peak at 772 cm^{-1} is indicative for the incoming of the all-trans planar zigzag conformation.

In the previous section it was noticed that, after recrystallization into the β-phase, two broad X-ray diffraction peaks centered around $2\theta = 3.7°$ and 8.0° appear (see Figure 10b). Polymerization of the methacrylate monomers can be monitored by the C═C stretching band at 1631 cm^{-1}. When focusing on the spectral region 1550−1750 cm^{-1} (see Figure 11c) it is observed that the 1631 and 1720 cm^{-1} peak intensities decrease compared to the peak at 1600 cm^{-1} during the heating run. The peak at 1600 cm^{-1} is associated with the phenyl rings of syndiotactic polystyrene and can be considered as an internal reference. The C═C peak at 1631 cm^{-1} and the C═O peak at 1720 cm^{-1} originate from cyclohexyl methacrylate. The intensity of the C═C stretching band decreases more in comparison to the C═O peak, indicating that cyclohexyl methacrylate polymerizes during the heating run up to T = 210 °C. Since Raman measurements have been performed simultaneously with SAXS and WAXS, the appearance of the two broad X-ray diffraction peaks must be a result of thermal polymerization, an error that occurred in our experimentation due to improper addition of inhibitor but was of use for the sPS/CHMA system. These findings are in accordance with the X-ray diffraction data of poly(cyclohexyl methacrylate) (PCHMA), which shows two broad reflections, one at the higher angles originating from the van der Waals interaction between the cyclohexyl rings and the other less intense reflection at lower angles originating from the separation of the chain segments, i.e., the average distance between adjacent main chains,[33] similar to atactic polystyrene.[34]

On continued heating, the WAXS results demonstrate that above a temperature of T = 210 °C, the reflections at $2\theta = 3.7$ and 8.0° (d = 11.57 and 5.43 Å) disappear. In the same temperature region, changes in the spectral region from 1550 to 1800 cm^{-1} of the Raman spectra are observed. While on polymerization the intensities of the peaks at 1631 and 1720 cm^{-1} decrease compared to 1600 cm^{-1}, now, it is observed that the intensities of the peaks increases again. This shows that the polymer depolymerizes upon further heating. The consequence of the depolymerization is that the WAXS reflections at $2\theta = 3.7$ and 8.0° disappear. These observations are associated with the ceiling temperature of cyclohexyl methacrylate,[35] a subject that is out of the scope of the

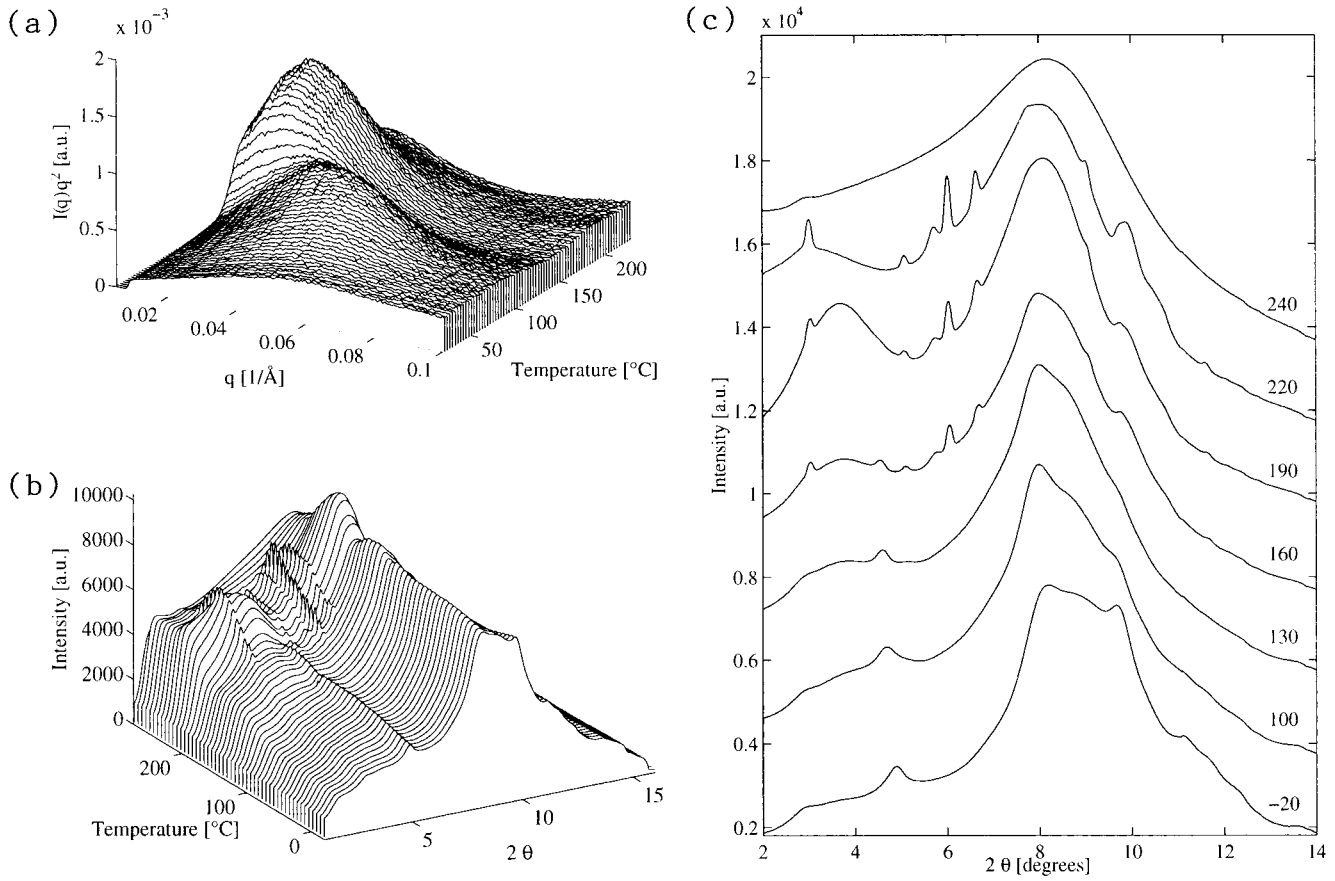

Figure 10. Heating run of a quenched 40 wt % sPS/CHMA sample: (a) 3-D plot of SAXS data from 20 to 230 °C at 5 °C/min; (b) 3-D plot of WAXS data from −20 to +230 °C at 5 °C/min; (c) 2-D plot of WAXS data (temperatures are indicated in the plot).

present paper. Polymerization of these reactive solvents and their influence on the formation of sPS-polymerized solvent intercalates will be discussed in a subsequent paper.[36]

V. Discussion

The results presented for the different sPS/solvent systems show the presence of a polymer/solvent compound in the helical phase and its transformation into a planar zigzag phase on heating. This is in agreement with results reported by other authors. However, the observed structural changes, which occur in the helical phase on heating, are not in full agreement with the thus far reported δ- to γ-phase transformation. Therefore, the structural changes observed within the helical phase and the transformation of the helical to planar zigzag phase will be discussed separately in section V.A. Further, for the 20 wt % sPS/BzMA system, it was noticed that reflections associated with the β-phase appear and disappear at rather low temperatures. The metastability of these β-crystals will be discussed in section V.B. Finally, in section V.C, the sensitivity of the used experimental techniques summarizing the overall generality of the changes occurring in DSC, SAXS, WAXS and Raman spectroscopy will be discussed in view of the applicability in gel studies.

A. Structural Changes on Heating. Structural Order of the Solvent in the Helical Phase. The observations made by WAXS during the heating runs on the investigated sPS/solvent systems revealed the presence of different structures within the helical phase (see Figures 3, 4, 6, 8, and 10 for the sPS/decalin, sPS/BzMA and sPS/CHMA systems). It was also observed that in the quenched samples the positions of the reflections assigned to the helical δ-phase depend on the solvent (see Tables 2, 4, and 5). Since this helical phase is known to be a compound between the polymer and the solvent, the structure of the helical phase is dependent on the size and structure of the solvent molecules. Because of the molar volume of the solvent molecules, it is anticipated that the δ-phases of sPS/BzMA, sPS/CHMA, and sPS/decalin should have a more open structure than sPS/toluene[37] and sPS/ethylbenzene.[29] From Tables 2, 4, and 5, it is evident that indeed the structure is more "open" along the *b*-axis as seen from the position of the 010 reflection, whereas the structure along the *a*-axis remains more or less unaltered (indifferent of solvent). This suggests that the solvent mainly affects the *b*-axis of the unit cell. Since the δ-phase is known to be a compound, the solvent molecule should always be positioned along the *b*-axis independent of its structure. Whereas along the *a*-axis right-handed and left-handed polymer chains align alternately, they come into contact at the van der Waals distances. Therefore no additional space is available to accommodate a guest molecule along the *a*-axis.[37]

On heating the quenched samples of the sPS/BzMA above a temperature of 50 °C, two broad reflections centered around $2\theta = 3.6°$ ($d = 12.05$ Å) and 8.8° ($d = 4.91$ Å) are observed (see Figures 6 and 8), while the other reflections remain the same. These broad reflections are more pronounced for the 20 wt % sPS/BzMA system. Similar broad reflections are also observed for the sPS/CHMA system (see Figure 10). The absence of these reflections in the sPS/decalin systems (see Figures 3 and 4) indicates that these reflections are specific for

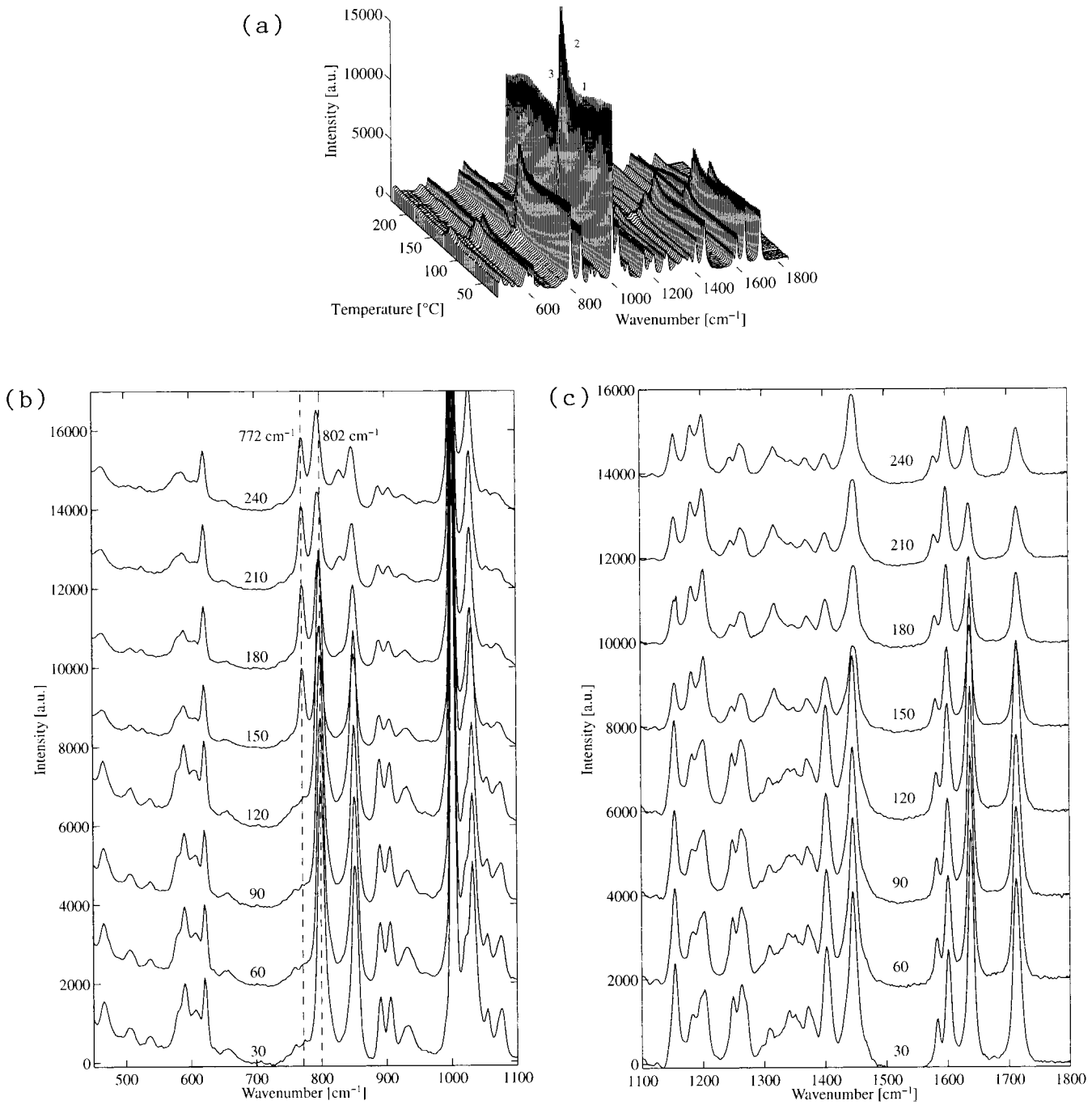

Figure 11. Heating run from 20 to 230 °C at 5 °C/min of a quenched 40 wt % sPS/CHMA sample: (a) 3-D plot of Raman data; (b) 2-D plot of Raman data in region 450-1100 cm^{-1}; (c) 2-D plot of Raman data in region 1100−1800 cm^{-1}. Temperatures are indicated in plots b and c. Markers 1−3 indicate temperatures of 90, 100, and 150 °C, respectively.

the solvent. The corresponding *d* values of these reflections, 12.05 and 4.91 Å respectively, are equal to the dimensions of the BzMA molecule. The dimensions of the molecular structures of the different solvents used were shown in Figure 1. From this, it is clear that the reflections at $2\theta = 3.6$ and 8.8° originate from the regular packing of the BzMA molecules within the confined spaces of the helical structure of sPS. The observed *d* values are in close accordance with the local order as observed in poly(benzyl methacrylate), where the reflection at lower angles (*d* spacing is 11.0 Å) is attributed to the order between the adjacent main chains and the reflection at higher angles (*d* spacing is 5.0 Å) is associated with order between the phenyl rings arising from the van der Waals interactions.[33] The similarities in the *d* values for both the monomer in the compound and the pure polymer poly(benzyl methacrylate) indicates that a similar local order as observed for PBzMA exists in the BzMA molecules intercalated within the helices of sPS. This could only be feasible when the phenyl rings of BzMA are intercalated between the phenyl rings of sPS in the same chain along the *b*-axis. The structure of the sPS/BzMA compound is rather different from the sPS/toluene compound. As discussed by Chatani et al.[37] in sPS/toluene, the solvent molecules occupy the isolated holes between the polymer chains along the *b*-axis of the unit cell. Each toluene molecule is surrounded by 10 polymer phenyl rings, as shown schematically in Figure 3 of ref 37. The model for sPS/BzMA polymer/solvent compounds will be discussed in more detail in a subsequent paper.[36]

A closer investigation of the WAXS data of the sPS/CHMA system shows that the structure of the compound is similar to that for sPS/BzMA. On the other hand, for decalin, we only observe a single, strong reflection at $2\theta = 8.0°$, originating from the order present between the alkyl rings, which arises from van der Waals interaction between the molecules. No order between the adjacent molecules exists.

Structural Disorder of the Solvent in the Helical Phase. As evident from Figures 6 and 8, the packing of the solvent molecules, which seems initially absent due to the fast quenching, becomes more regular within the δ-phase on heating. Besides the regular ordering of the solvent molecules within the δ-phase, the WAXS observations also showed that structural changes occur within the helical phase on further heating. The occurrence of changes within the helical phase was also observed for many other sPS/solvent systems, and these changes were related to desiccation of the solvent from the helices, resulting in the solvent-free γ-phase.[12,29] What follows are the highlights of the experimental observations made earlier and the implications on the present study. More elaborate studies on the δ- to γ-transition have been carried out by Chatani et al.,[37] Wang et al.,[29] and De Candia et al.[38] Chatani et al. demonstrated that in sPS/toluene systems during the transformation from the δ- to γ-phase, the *b*-axis of the helical phase decreases by approximately 2 Å, while the *a*-axis is retained.[37] This indicates that the unit cell is re-formed during the transition into a more dense packing. The assignment of the 010 and 200 reflections, as used by Wang et al.,[29] and their experimental results on sPS/ethylbenzene are consistent with the model that the unit cell shrinks along the *b*-axis upon decomplexation, though they also observed a minor change in the dimensions of the *a*-axis. The study of De Candia et al.[38] were in line with the previous, but they suggested that the transition from the δ- to γ-transition occurs via the formation of an intermediate mesomorphic phase.

As shown in section IV.B on the results from the sPS/BzMA systems, the two reflections assigned to BzMA disappear, when the structural changes within the helical phase set in. This can be interpreted either as desiccation of the solvent molecules out of the interstitial regions of the helices leading to the formation of the γ-phase or as a loss in the packing of solvent molecules within the confined space. If the former is true, we would anticipate a decrease of the unit cell dimensions on the δ- to γ-transition, while this would not be the case in the latter, where the solvent molecules are intercalated within the helix. To reach to a conclusion, a more detailed analysis of the 010 and 200 reflections of the δ-phase is made.

The 010 reflection at $2\theta = 2.9°$ ($d = 15.17$ Å) remains more or less constant during heating, whereas the 200 reflection at $2\theta = 5.1°$ ($d = 8.59$ Å) shows a gradual shift to lower angles during the structural changes within the helical phase. The fact that the 010 reflection stays at the same position and the 200 reflection shifts to lower angles indicates that no contraction of the unit cell occurs. This implies that the solvent resides within the helices. The disappearance of the reflection at $2\theta = 3.6°$ ($d = 12.05$ Å) shows that the order between the adjacent solvent molecules is lost. Simultaneously, changes are observed in the reflection at $2\theta = 8.8°$ ($d = 4.91$ Å). This suggests that the observed changes are related to the van der Waals interactions between the phenyl rings. Besides the gradual shift of the 200 reflection, the sharpness of this reflection broadens. This shows that the packing of the polymer chains in the helical phase becomes less regular. At the same time, a sharp reflection at $2\theta = 8.0°$ ($d = 5.45$ Å) appears.

Table 6. Diffraction Angles (deg) and Bragg Distances (Å) Observed in the WAXS Spectra for the 40 wt % sPS/BzMA System: the δ'- versus δ''-Phase

hkl	d_{obs}	$2\theta_{obs}$	phase
010	15.17	2.86	δ'
200	8.59	5.05	δ'
	4.50	9.66	δ'
	3.90	11.14	δ'
	3.76	11.57	δ'
	3.54	12.27	δ'
	3.18	13.67	δ'
010	15.17	2.86	δ''
200	9.39	4.62	δ''
	5.45	7.97	δ''
	4.88	8.89	δ''
	4.48	9.69	δ''
	3.91	11.11	δ''
	3.50	12.41	δ''

The appearance of a sharp reflection around $2\theta = 8.0°$ ($d = 5.45$ Å) and the disappearance of the broad reflection at $2\theta = 3.6°$ ($d = 12.05$ Å) and the simultaneous shift of the reflection at $2\theta = 8.8°$ (d = 4.91 Å) can be explained by the change in the order of the solvent structure. The sharp reflection at $2\theta = 8.0°$ seems to originate from the ordering of the phenyl rings of the sPS chains alone (here the packing of the phenyl rings is more regular due to the covalent bonds), rather than the ordering of the intercalated phenyl rings between BzMA and sPS as observed at lower temperatures. The sharpness of the new reflection at $2\theta = 8.0°$ suggests a better packing of the phenyl rings of sPS rather than the van der Waals interaction between the intercalated phenyl rings of sPS and BzMA. The small shift of the broad reflection at $2\theta = 8.8°$ to higher angles such as 8.9° ($d = 4.88$ Å) should be related to interactions between phenyl rings of BzMA. From these observations, it is evident that a distinction has to be made within the δ-phase based on the structural (dis)order of the solvent molecules within the confined spaces of the sPS helices.

From here on, the δ-phase in which the solvent molecules are ordered will be referred to as the δ'-phase, whereas the δ-phase in which the solvent molecules are disordered will be referred to as the δ''-phase. The reflections associated with these phases are given in Table 6.

Our observations are different from the results published by the other authors, who performed their studies at room temperature after desiccation of the solvent from the δ-phase, which results in the formation of the γ-phase. Thus as anticipated, they observed a decrease in the unit cell dimensions in the γ-phase, which they referred to as the solvent-free phase. This is in contrast to the expansion of the helical phase during the δ' to δ'' transition, as observed in situ in our study. Unlike the solvent-free γ-phase observed by the other authors, we have a helical phase, δ'', in which the solvent is still present within the helical phase of sPS, though the structural order between the adjacent solvent molecules to a great extent is lost.

In the quenched sample of sPS/CHMA, the δ'- and the δ''-phase coexist unlike in the sPS/BzMA system,

where a pure δ'-phase could be obtained (see Table 6). Considering the intensity of the reflection for the δ''-phase, it appears that the δ''-phase predominates in the quenched sample. On heating, the transformation from δ' to δ'' could be noticed from the disappearance of the reflection at $2\theta = 9.7°$ ($d = 4.50$ Å), which is associated with the δ'-phase, and the strengthening of the reflection at $2\theta = 8.0°$ ($d = 5.45$ Å), which is associated with the δ''-phase (see Figure 10). Changes within the helical phase (δ' to δ'') may also be noticed for the sPS/decalin systems. This is evident from the changes of the 200 reflection during the phase transformation (see Table 2 and Figures 3 and 4).

From here, it is evident that the transformation within the helical phase is independent of the solvent and thus is a general feature to be observed for sPS/solvent systems—in all systems where the solvent is not desiccated.

Helical to Planar Zigzag Transition via a Melting and Recrystallization Process and the Formation of the β-Phase. The DSC traces in Figures 5 and 9 for the sPS/BzMA and sPS/CHMA systems, respectively, show an endotherm at 130 °C. From WAXS we noticed the disappearance of the reflections of the δ''-phase. Therefore, the endotherm can be interpreted as melting of the δ''-phase. On continued heating, an onset of an exotherm observed at 135 °C indicates crystallization in the β-phase, as observed by WAXS. The morphological changes during the melting of the δ''-phase and the crystallization of the β-phase have been followed by simultaneous SAXS. In Figures 3, 4, 6, 8, and 10 for sPS/decalin, sPS/BzMA, and sPS/CHMA systems, this is observed first as a decrease in intensity followed by an increase and a subsequent shift of the maximum to lower angles. Once the transformation into the β-phase occurs, a lamellar morphology will set in as earlier investigated by transmission electron microscopy.[29] The resultant maximum in the SAXS pattern corresponds to the average lamellar thickness. The shift in the SAXS maximum to lower angles on further heating corresponds to the anticipated increase in the lamellar thickness. Continued heating results in a drop in intensity due to melting of the lamellae.

The drop in the intensity followed by an increase of the intensity together with the shift to lower angles is a common feature for all systems. For a detailed analysis, we will investigate the SAXS results for the 40 wt % sPS/decalin system (Figure 4). With the help of the changes in the SAXS invariant Q, occurring during heating, we can follow the electron density fluctuations during the phase transformation. The invariant Q is defined as

$$Q = \int_0^\infty q^2 I(q)\, \mathrm{d}q$$

where $I(q)$ is the intensity and q is the scattering vector. The changes in the invariant as function of temperature for the 40 wt % sPS/decalin system are well illustrated in Figure 12. The invariant shows, after reaching a maximum at 100 °C, a large drop up to 140 °C. This drop occurs because of the homogenization of polymer in the solvent, leading to a decrease in electron density fluctuations during the melting of the helical phase. The subsequent increase of the invariant is a result of recrystallization into the β-phase. This further demonstrates that the transformation from δ'' to β occurs via a melting and recrystallization process.

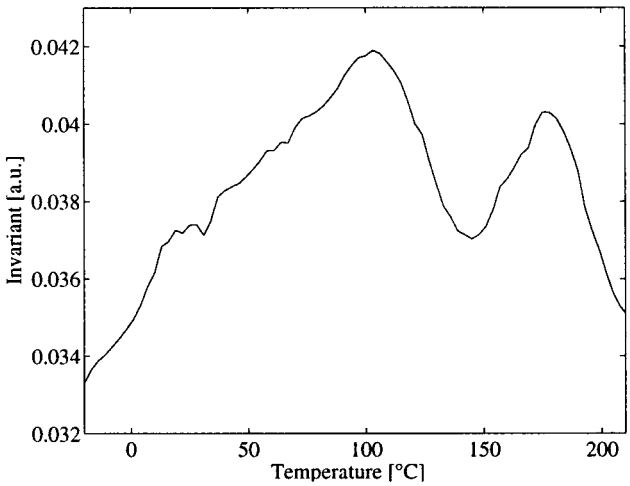

Figure 12. SAXS invariant during a heating run from −20 to +230 °C at 5 °C/min of a quenched 40 wt % sPS/decalin sample.

B. Metastability of the β-Phase. In section IV.B on the results of in situ WAXS of the 20 wt % sPS/BzMA system, the appearance and disappearance of the β-phase, i.e., the metastability of the β-phase, was observed together with the helical (δ') to helical (δ'') transformation. The metastability of the β-phase was only observed for the 20 wt % sPS/BzMA system.

A possible explanation for this metastability can be as follows. As known, during quenching of the homogeneous solution, the sPS chains adopt a helical conformation in the δ-phase, resulting in macroscopic gelation, leading to polymer rich domains, mainly in the helical δ-phase, and solvent rich domains. The polymer rich domains are connected to each other by polymer chains in the solvent rich domains. The incoming of the β-phase with the δ' to δ'' phase transformation in the low polymer concentration (20 wt % sample) suggests a direct transformation from the δ'- to β-phase, the β-phase being the thermodynamically most stable phase. Since the formation of the β-phase can only occur via a melting and recrystallization process, the melting (or randomization) of the chains can be achieved easily in the solvent rich domains. This cannot be realized in the 40 wt % sPS system, because in the 40 wt % sPS system the volume fraction of solvent rich domains is much less compared to that in the 20 wt % sPS system. The crystallization of the β-phase in the solvent rich domains is further favored because of high supercoolings at this temperature, leading to the formation of small crystals. Because of the small crystal dimensions and the imperfection within the crystals formed due to the anticipated fast growth rate at the large supercoolings, these crystals will tend to dissolve on further heating, which is indicative of the metastable state of these crystals.

C. Sensitivity of the Techniques Used. From the results presented above, it is evident that X-ray investigations using synchrotron radiation is a powerful tool to follow structural and morphological changes in real time, even in relatively low polymer concentration polymer/solvent systems. Thus, it gives a new leverage in gel studies in general. In this section, we would like to scrutinize our results by taking into account the limitations of the individual techniques used in this study. This applies to all systems studied in the present work.

With DSC, it is only possible to measure the heat absorbed during melting of the helical phase and heat evolved during recrystallization to the planar zigzag phase. However, no heat effects, if there are any, during the helical (δ') to helical (δ'') phase transformation could be observed. Similarly, Raman spectroscopy also seems to be ineffective to follow this phase transformation, given the experimental setup used in the present study. But, changes in the scattering power of the sample during the phase transformation could be detected via the backscattered intensity in the Raman spectroscopy. In this respect, WAXS proves to be a more valuable technique, since it can give insight into the subtle changes occurring during this transformation, like ordering or disordering of the intercalated solvent molecules within the helices.

From the WAXS results, it would have been interpreted that the helical to planar zigzag transformation occurs gradually. The same holds for the results from Raman spectroscopy. But the simultaneously obtained SAXS data show that the long range is lost during this transformation. Consequently, this transformation results in a dip in the SAXS intensity, i.e., a drop in the electron density fluctuations, due to the homogenization during melting, as seen more pronounced by the SAXS invariant (the integrated intensity). The combination of SAXS, WAXS, and Raman spectroscopy shows that during this melting process, though the long-range order is lost, the short-range order is maintained to a great extent.

WAXS showed that during crystallization into the β-phase the intensities of the associated reflections increase. This is in accordance with the observed exotherm in the DSC. The simultaneously obtained SAXS data also show an increase in intensity followed by a shift to lower angles. These results suggest that during the overall crystallization process, crystals also thicken.

The melting behavior of the β-phase is observed in DSC by two endotherms, which may be interpreted as melting of crystals with two different crystal thicknesses (in average) or as melting of thinner crystals followed by crystallization into thicker crystals. For the investigated systems, such a complicated melting behavior could not be followed by SAXS/WAXS and Raman spectroscopy. SAXS seems to be insensitive to following such changes due to the large width of the reflection observed of these temperatures. WAXS only shows a continuous decrease during the melting of the crystals in the β-phase. Similarly, the intensities of the conformational bands in the Raman spectra also show a gradual decrease. However, the backscattered intensity of the Raman spectroscopy shows a sudden increase in intensity at the same temperatures as the endotherms observed by DSC, due to the changes in the scattering power during the melting process. The fact that the intensity increases rather than drops suggests that the melting process involves melting of crystals with two different crystal thicknesses and that in these particular systems the melting does not proceed via the melting and recrystallization process.

From the DSC alone, it would have been concluded that there is no difference in the phase behavior between sPS/BzMA and sPS/CHMA systems. But the combination of the techniques does show the differences, as summarized above. SAXS/WAXS/Raman spectroscopy performed simultaneously further strengthens the interpretation of the results.

VI. Concluding Remarks

In this paper the phase behavior of sPS with different solvents, i.e., decalin, benzyl methacrylate, and cyclohexyl methacrylate, was discussed. These polymer/solvent combinations were used as a model study to investigate the miscibility and the interaction of the solvent with sPS. The observed compound formation between sPS and reactive solvents (monomers) could lead, after polymerization, to unique polymer blend systems. Polymerization studies of sPS/reactive solvent (monomer) compounds will be presented in a subsequent paper.[35] From the presented results the following conclusions can be drawn:

(1) The sPS/solvent systems clearly demonstrate that in the quenched samples compound formation occurs, resulting in the known δ-phase, i.e., the solvent-included helical phase.

(2) Within the δ-phase, the solvent is intercalated between the phenyl rings of the helices. Between the solvent molecules, structural order or disorder can be present, leading to two different modifications of the δ-phase, termed as δ' and δ'', respectively. A detailed model will be presented in a subsequent paper.[36]

(3) The phase transformation from δ' (structural order between the solvent molecules) to δ'' (structural disorder between the solvent molecules) occurs on heating.

(4) The interaction between the phenyl rings of the solvent and sPS plays a prominent role in the existence of the δ'- and δ''-phases.

(5) Unlike the known δ (solvent-included phase) to γ (solvent-free phase) transformation on heating, no solvent-free γ-phase was observed in our studies. The absence of the γ-phase in our studies indicates that the formation of the γ-phase is purely a result of the desiccation process of the solvent.

(6) The transformation from the helical (δ'') to the planar zigzag (β) occurs via a melting and recrystallization process. During the melting process, while the morphological long-range order is lost, the short-range order between the neighboring polymer chains remains to some extent.

(7) Under specific conditions, the β-phase, which is thermodynamically the stable phase can appear as a metastable phase.

(8) The combination of used techniques, especially the simultaneous SAXS/WAXS/Raman spectroscopy, is a powerful tool to follow the morphological, structural, and conformational changes in polymer/solvent gels.

(9) From DSC, the phase diagrams of sPS/BzMA, sPS/CHMA, and sPS/decalin may appear to be the same. But, structural differences within the helices exist depending on the interaction between the polymer and solvent.

Acknowledgment. The authors are indebted to the CLRC Daresbury Laboratory for the research and travel grant to perform the combined SAXS and Raman spectroscopy experiments. The authors would like to thank Ernie Komanschek and Anthony Gleeson for the technical support on beamline 8.2 of the SRS. The Kaiser Holoprobe system was kindly loaned by Dr. John Andrews of Clairet Scientific, U.K. Further, the authors are grateful for the availability of the facilities at Beamline ID-11/BL-2 of the European Synchrotron Radiation Facility (ESRF), Grenoble, France. Especially

the support of Heinz Graafsma during the experiments is acknowledged, together with the assistance of Andy Hammersley in the analysis of the data with the help of the FIT2D software program, developed at ESRF. DOW Terneuzen is acknowledged for supplying syndiotactic polystyrene.

References and Notes

(1) Ishihara, N.; Seimiya, T.; Kuramoto; M.; Uoi; M. *Macromolecules* **1986**, *19*, 2464.
(2) Natta, G.; Pino, P.; Corradini, P.; Danusso, F.; Mantia, E. *J. Am. Chem. Soc.* **1955**, *77*, 1700.
(3) Venderbosch, R. W.; Meijer, H. E. H.; Lemstra, P. J. *Polymer* **1994**, *35*, 4349.
(4) Venderbosch, R. W.; Meijer, H. E. H.; Lemstra, P. J. *Polymer* **1995**, *36*, 1167.
(5) Goossens, J. G. P.; Rastogi, S.; Meijer, H. E. H.; Lemstra, P. J. *Polymer*, in press.
(6) Natta, G.; Danusso; F.; Moraglio, G. *Makromol. Chem*. **1958**, *28*, 166.
(7) Nakaoki, T.; Kobayashi, M. *J. Mol. Struct.* **1991**, *242*, 315.
(8) Chatani, Y. *J. Polym. Sci., Polym. Phys.* **1991**, *29*, 1649.
(9) Girolamo, M.; Keller, A.; Miyasaka, K.; Overbergh, N. *J. Polym. Sci., Polym. Phys. Ed*. **1976**, *14*, 39.
(10) Immirzi, A.; De Candia, F.; Iannelli; P.; Vittoria, V.; Zambelli, A. *Makromol. Chem., Rapid Commun*. **1988**, *9*, 761.
(11) Chatani, Y.; Fujii, Y.; Shimane, Y.; Ijitsu, T. *Polym. Prepr. Jpn. (Engl. Ed.)* **1988**, *37*, E248.
(12) Guerra, G.; Vitagliano, V. M.; De Rosa, C.; Petraccone, V.; Corradini, P. *Macromolecules* **1990**, *23*, 1539.
(13) Greis, O.; Asano, T.; Xu, Y.; Petermann, J. *Z. Kristallogr.* **1988**, *182*, 58.
(14) Greis, O.; Xu, Y.; Asano, T.; Petermann, J. *Polymer* **1989**, *30*, 590.
(15) Guenet, J. M. *Macromolecules* **1986**, *19*, 1961.
(16) Keller, A. *Faraday Discuss.* **1996**, *34*, 1.
(17) Deberdt, F.; Berghmans, H. *Polymer* **1993**, *34*, 2192.
(18) Deberdt, F.; Berghmans, H. *Polymer* **1994**, *35*, 1694.
(19) Roels, T.; Rastogi, S.; De Rudder, J.; Berghmans, H. *Macromolecules* **1997**, *30*, 7939.
(20) Kobayashi, M.; Nakaoki, T.; Ishihara, N. *Macromolecules* **1990**, *23*, 78.
(21) Kobayashi, M.; Kozasa, T. *Appl. Spectrosc.* **1993**, *47*, 1417.
(22) Kellar, E. J. C.; Galiotis, C.; Andrews, E. H. *Macromolecules* **1996**, *29*, 3515.
(23) Roels, T.; Deberdt, F.; Berghmans, H. *Macromolecules* **1994**, *27*, 6216.
(24) Daniel, C.; Deluca, M. D.; Guenet, J. M.; Brulet, A.; Menelle, A. *Polymer* **1996**, *37*, 1273.
(25) Bras, W.; Derbyshire, G. E.; Ryan, A. J.; Mant, G. R.; Felton, A.; Lewis, R. A.; Hall, C. J.; Greaves, G. N. *Nucl. Instrum. Methods, Phys. Res. A* **1993**, *A326*, 587.
(26) Everall, N.; Owen, H.; Slater, J. *Appl. Spectrosc.* **1995**, *49*, 610.
(27) Bryant, G. K.; Gleeson, H. F.; Ryan, A. J.; Bogg, D.; Goossens, J. G. P.; Bras, W. Submitted to *Rev. Sci. Instrum*.
(28) Berghmans, H.; Deberdt, F. *Philos. Trans. Soc. London A.* **1994**, *348*, 117.
(29) Wang, Y. K.; Savage, J. D.; Yang, D. C.; Hsu, S. L. *Macromolecules* **1992**, *25*, 3659.
(30) Kobayashi, M.; Nakaoki, T.; Ishihara, N. *Macromolecules* **1989**, *22*, 4377.
(31) Filho, A. R.; Vittoria, V. *Makromol. Chem., Rapid Commun.* **1990**, *11*, 199.
(32) Reynolds, N. M.; Stidham, H. D.; Hsu, S. L. *Macromolecules* **1991**, *24*, 3662.
(33) Miller, R. L.; Boyer, R. F.; Heijboer, J. *J. Polym. Sci., Polym. Phys. Ed.* **1984**, *22*, 2021.
(34) Mitchell, G. R.; Windle A. H. *Polymer* **1984**, *25*, 906.
(35) Corstjens et al. Manuscript in preparation.
(36) Rastogi, S.; Goossens, J. G. P.; Lemstra, P. J. Manuscript in preparation.
(37) Chatani, Y.; Shimane, Y.; Inagaki, T.; Ijitsu, T.; Yukinari, T.; Shikuma, H. *Polymer* **1993**, *34*, 1620.
(38) De Candia, F.; Guadagno, L.; Vittoria, V. *J. Macromol. Sci., Phys. Ed.* **1995**, *B34*, 95.

MA9712920